Implementation Aspects of Nonlinear Precoding for G.fast - Coding and Legacy Receivers

Rainer Strobel‡, Andreas Barthelme*, Wolfgang Utschick*
*Professur für Methoden der Signalverarbeitung, Technische Universität München, 80333 München, Germany
{a.barthelme,utschick}@tum.de
‡Intel Connected Home Division, 85579 Neubiberg, Germany, rainer.strobel@intel.com

***Abstract*—Hybrid copper/fiber networks bridge the gap between the fiber link at the distribution point and the customer by using copper wires over the last meters. The G.fast technology has been designed to be used in such a fiber to the distribution point (FTTdp) network. Crosstalk management using MIMO precoding is a key to the required performance of FTTdp. With higher frequencies used on copper wires, nonlinear precoding schemes such as Tomlinson Harashima precoding are discussed as an alternative to linear precoding. This paper focuses on the advantages and losses of Tomlinson Harashima precoding used for coded transmission on twisted pair cable bundles. A performance loss model for the Modulo loss in coded transmission is presented. Interoperability between linear and nonlinear precoding is discussed.**

I. Introduction

While the first generation of G.fast-based broadband Internet access systems using 106 MHz bandwidth becomes more stable and first field deployments are starting, G.fast extensions towards higher frequencies are discussed. Tomlinson-Harashima precoding (THP) is discussed as a potential replacement of linear precoding (LP) for crosstalk management at frequencies beyond 106 MHz. While the performance benefits of THP over LP for uncoded transmission on high crosstalk channels are known, this performance benefit is not necessarily present in typical G.fast scenarios [1]. Performance penalties due to certain implementation aspects are investigated for a realistic view on the potential gains on nonlinear precoding.

Joint precoding of linear and modulo receivers is needed in cases where legacy equipment without modulo receivers coexists with equipment supporting THP signals. This paper presents an approach to modify the THP structure to support linear and modulo receivers in the same precoding group.

II. System Model

THP is discussed as a potential precoding method to be used for 212 MHz G.fast in high crosstalk environments. 212 MHz-G.fast uses the same carrier spacing as 106 MHz (51.75 kHz) and increases the number of carriers to $K = 4096$. TH precoding requires modulo receivers at the CPE side to decode the signals. The modulo receiver may receive signals from linear and TH precoded DPUs, but comes with some performance penalty.

A. Architecture

Downstream transmission with THP and modulo receivers for one carrier $k = 1,\ldots,K$, as in Fig. 1, performs the processing steps according to

$$\boldsymbol{u}_{\text{back}}^{(k)} = \boldsymbol{S}^{(k),-1}\boldsymbol{B}^{(k)}\boldsymbol{u}_{\text{mod}}^{(k)}, \tag{1}$$

$$\boldsymbol{u}_{\text{mod}}^{(k)} = \boldsymbol{S}^{(k)}\text{mod}\left(\boldsymbol{u}_{\text{back}}^{(k)} + \boldsymbol{u}^{(k)}\right), \tag{2}$$

$$\hat{\boldsymbol{u}}^{(k)} = \text{mod}\left(\boldsymbol{S}^{(k),-1}\boldsymbol{G}^{(k)}\left(\boldsymbol{H}^{(k)}\boldsymbol{P}^{(k)}\boldsymbol{u}_{\text{mod}}^{(k)} + \boldsymbol{n}^{(k)}\right)\right). \tag{3}$$

The transmit signal $\boldsymbol{u}^{(k)}$, created by quadrature amplitude modulation (QAM), is gain-scaled by the diagonal matrix $\boldsymbol{S}^{(k)}$. A feed-back signal $\boldsymbol{u}_{\text{back}}^{(k)}$ is calculated according to Eq. (1), using the strictly lower triangular feedback matrix $\boldsymbol{B}^{(k)}$ and a modulo operation $\text{mod}\ (.)$ [2]. The resulting signal

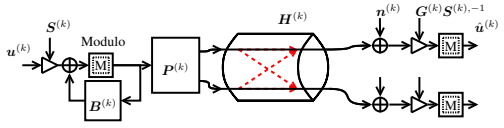

Fig. 1. Downstream system model representing one subcarrier

$\boldsymbol{u}_{\text{mod}}^{(k)}$ is further processed by multiplication with the precoder matrix $\boldsymbol{P}^{(k)}$ and transmitted over the channel, represented by $\boldsymbol{H}^{(k)}$. At the receiver side, the signal experiences additive white Gaussian zero-mean noise $\boldsymbol{n}^{(k)} \sim \mathcal{N}\left(\boldsymbol{0}, \sigma^2\boldsymbol{I}\right)$. The receive signal is scaled by the inverse transmit gain $s_l^{(k),-1}$ and the frequency domain equalizer $g_l^{(k)}$. The equalized signal is processed by the QAM demodulator.

As this paper investigates coding and decoding aspects, the encoder and decoder blocks are considered. G.fast uses two codes for error correction, an outer Reed-Solomon (RS) block code and an inner convolutional code, the 4D-Wei-code [3].

B. Theoretical View on THP

Tomlinson Harashima precoding is an approximation of the optimal coding scheme, dirty paper coding (DPC) [4]. From a channel capacity perspective [5], nonlinear precoding gives advantages over linear precoding. Compared to dirty paper coding, practical implementations of nonlinear precoding such as THP come with some losses due to the transmitter and receiver side modulo operations. From literature, e.g. [6], three types of losses are known for THP, shaping loss, power loss and modulo loss. Shaping loss is the difference between the capacity achieved by the optimal (Gaussian) modulation alphabet and the uniformly distributed modulation alphabet,

ISBN 978-0-9928626-7-1 © EURASIP 2017

which is a result of the transmitter side modulo operation. In G.fast, this applies to both, linear and nonlinear precoding, because a QAM modulation is used for both, linear and nonlinear precoding. Therefore, it is not discussed.

The power loss caused by the transmitter-side modulo operation as well as the modulo loss caused by the receiver-side modulo operation are relevant for the THP implementation.

III. Precoder-Side Implementation Aspects

At the downstream transmitter side, power constraints must be satisfied and therefore, the power loss must be considered. Besides that, legacy receivers have to be taken into account.

A. Power Constraints and Power Loss

Precoding and spectrum optimization for G.fast are subject to transmit power constraints. Rate maximization for THP is discussed in [1], where the power loss of THP is represented by a diagonal gain matrix $\boldsymbol{P}_{\mathrm{m}}^{(k)}$ in the power constraints, which is derived from the precoder signals or from the bit allocation.

For G.fast, the per-line spectral mask constraint,

$$\left(\boldsymbol{P}^{(k)}\boldsymbol{P}_{\mathrm{m}}^{(k)}\right)\odot\left(\boldsymbol{P}^{(k)}\boldsymbol{P}_{\mathrm{m}}^{(k)}\right)^{*}\boldsymbol{x}^{(k)}\leq\boldsymbol{p}_{\mathrm{mask}}^{(k)}\forall k=1,\ldots,K \quad (4)$$

and the per-line sum-power constraint,

$$\sum_{k=1}^{K}\left(\boldsymbol{P}^{(k)}\boldsymbol{P}_{\mathrm{m}}^{(k)}\right)\odot\left(\boldsymbol{P}^{(k)}\boldsymbol{P}_{\mathrm{m}}^{(k)}\right)^{*}\boldsymbol{x}^{(k)}\leq\boldsymbol{p}_{\mathrm{sum}} \quad (5)$$

apply. $\boldsymbol{x}^{(k)}$ is the transmit power vector for carrier k, $x_l^{(k)}=|s_l^{(k)}|^2$ and $\odot$ denotes the Hadamard product, i.e., the element-wise product of the matrices, $\boldsymbol{p}_{\mathrm{mask}}^{(k)}\in\mathbb{R}^L$ is the per-carrier power limit, derived from the spectral mask constraint and $\boldsymbol{p}_{\mathrm{sum}}\in\mathbb{R}^L$ is the vector of per-line sum-power limits.

Power loss exists, because the signal at the output of the modulo operation (Eq. (2)) is approximately uniformly distributed within the modulo region, while at the input, the signal consists of the QAM signal of the corresponding constellation. Power loss is the ratio between the power of the modulo output signal and the QAM signal $\mathrm{E}\left[|u_l|^2\right]/\mathrm{E}\left[|u_{\mathrm{mod},l}|^2\right]$. Assuming that the modulo output signal $\boldsymbol{u}_{\mathrm{mod}}^{(k)}$ is uncorrelated, the diagonal elements of the matrix $\boldsymbol{P}_{\mathrm{m}}^{(k)}$, $p_{\mathrm{m},ll}$ are selected with respect to the constellation size $\hat{b}_l^{(k)}$ of the corresponding line l and carrier k according to Tab. I [7].

Bits $\hat{b}_l$	1	2	3	4	5	6
$p_{\mathrm{m,wc},ll}$/dB	1.25	1.25	0.28	0.28	0.80	0.06
Bits $\hat{b}$	7	8	9	10	11	12
$p_{\mathrm{m,wc},ll}$/dB	0.68	0.02	0.66	0	0.65	0

TABLE I
Worst case power loss per G.fast constellation

Tab. I is the worst-case power loss for the corresponding constellation, derived from a uniform distribution of $\boldsymbol{u}_{\mathrm{mod}}$, which only applies for the latter encoded lines. Assuming uncorrelated unit power signals at the precoder input $\boldsymbol{C}_{uu}^{(k)}=\mathrm{E}\left[\boldsymbol{u}^{(k)}\boldsymbol{u}^{(k),\mathrm{H}}\right]=\boldsymbol{I}$ and the modulo output covariance matrix $\boldsymbol{C}_{u_{\mathrm{mod}}u_{\mathrm{mod}}}^{(k)}=\mathrm{E}\left[\boldsymbol{u}_{\mathrm{mod}}^{(k)}\boldsymbol{u}_{\mathrm{mod}}^{(k),\mathrm{H}}\right]$, the actual power loss per carrier k and line l is derived from the covariance matrices by

$$p_{\mathrm{m},,ll}=s_l^{-1}\sqrt{\left[\boldsymbol{C}_{u_{\mathrm{mod}}u_{\mathrm{mod}}}^{(k)}\right]_{\mathrm{ll}}}\leq p_{\mathrm{m,wc},\hat{b}}. \quad (6)$$

While Tab. I can be used as a worst case assumption for initialization, Eq. (6) can be used for refinement.

B. Legacy Receivers

106 MHz G.fast operates with linear precoding, and the same holds for the first generation of 212 MHz devices. The corresponding CPEs are not equipped with modulo receivers. As it is practically difficult to replace all legacy equipment, supporting legacy CPE devices in the precoding group is important for the introduction of THP.

One option of joint precoding for linear and modulo receivers with minimal changes to the THP structure is to leave out the modulo operation $\mod(.)$ for the legacy lines $l\in\mathbb{I}_{\mathrm{legacy}}$. This results in a higher signal power for the legacy line signals $u_{\mathrm{mod},l}, l\in\mathbb{I}_{\mathrm{legacy}}$, because the corresponding signal is calculated according to

$$u_{\mathrm{mod},l}^{(k)}=s_l^{(k)}\begin{cases}\mod\left(u_{\mathrm{back},l}^{(k)}+u_l^{(k)}\right) & \text{for } l\in\mathbb{I}_{\mathrm{m}}\\ \left(u_{\mathrm{back},l}^{(k)}+u_l^{(k)}\right) & \text{for } l\in\mathbb{I}_{\mathrm{legacy}}.\end{cases} \quad (7)$$

instead of Eq. (2). The precoder coefficients itself do not require changes compared to standard THP with this approach.

Spectrum optimization according to [1] is important for such a system due to the transmit power increase. In the coexistence case, $\boldsymbol{P}_{\mathrm{m}}^{(k)}$ is no longer a diagonal matrix. A signal-based estimation of the modulo output power is given from the correlation matrices $\boldsymbol{C}_{u_{\mathrm{mod}}u}=\mathrm{E}\left[\boldsymbol{u}_{\mathrm{mod}}^{(k)}\boldsymbol{u}^{(k),\mathrm{H}}\right]$, representing the correlation between input and output of the nonlinear operation and $\boldsymbol{C}_{u_{\mathrm{mod}}u_{\mathrm{mod}}}$, which gives $\boldsymbol{P}_{\mathrm{m}}^{(k)}$ according to

$$p_{\mathrm{m},vd}^{(k)}=\begin{cases}s_l^{(k),-1}\sqrt{[\boldsymbol{C}_{u_{\mathrm{mod}}u_{\mathrm{mod}}}^{(k)}]_{vd}} & \text{for } v=d, v\in\mathbb{I}_{\mathrm{m}}\\ 1 & \text{for } v=d, v\in\mathbb{I}_{\mathrm{legacy}}\\ s_l^{(k)-1}[\boldsymbol{C}_{u_{\mathrm{mod}}u}^{(k)}]_{vd} & \text{for } v\neq d.\end{cases} \quad (8)$$

The result can be used in the constraint set of Eq. (4) and (5) and spectrum optimization algorithms as described in [1] are applicable to the TH precoder which supports legacy receivers.

IV. Receiver-Side Implementation Aspects

The modulo loss is caused by the receiver-side modulo operation required to decode TH precoded signals. The increased bit error rate due to the modulo loss depends on the channel coding and modulation method. Therefore, the modulation and coding used for G.fast is investigated in more detail to derive general rules for modulo loss in coded THP systems.

A. QAM Modulation in G.fast

In G.fast, each of the DMT subcarriers is modulated with a specific QAM constellation between 1 bit and 12 bit constellation size $\hat{b}^{(k)}$. The constellation size is selected to achieve

ISBN 978-0-9928626-7-1 © EURASIP 2017

the target bit error rate with some margin. The number of bits $\hat{b}$ to be modulated on a specific carrier depends on the available SNR. A widely used approximation [8] to derive the bit allocation from the SNR $SNR_l^{(k)}$ is

$$\hat{b}_l(k) = \left\lfloor \log_2\left(1 + \frac{SNR_l^{(k)}}{\Gamma}\right)\right\rfloor. \quad (9)$$

where Γ is the SNR gap to capacity. It consists of the SNR gap for uncoded QAM modulation 9.8 dB [8], the coding gain γ_{coding} and the SNR margin γ_{margin} which gives $\Gamma = 9.8\,\text{dB} - \gamma_{\text{coding}} + \gamma_{\text{margin}}$. G.fast is designed for a target bit error rate (BER) of $p_{\text{error,target}} = 10^{-7}$, which will be achieved with $\gamma_{\text{margin}} = 0\,\text{dB}$ SNR margin.

Eq. (9) gives only a coarse estimate bit allocation achieving the target bit error rates and does not consider a modulo receiver. A more precise lower bound on the bit error rate is derived, taking the constellation shape into account.

B. Error Probabilities for Linear and Modulo Receivers

A lower bound on the uncoded QAM bit error rates is derived for linear and modulo receivers by considering only the bit errors caused by bit flips to directly neighboring constellation points.

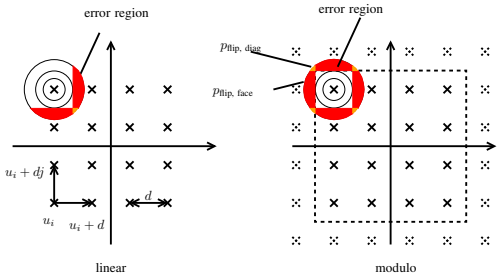

Fig. 2. Comparison of error regions with linear and modulo receiver

Assuming a Gaussian channel, where the desired signal u consists of the real part $u_{\text{re}} = \Re\{u\}$ and the imaginary part $u_{\text{im}} = \Im\{u\}$, the receive signal with additive noise is $\hat{u}_{\text{re/im}} \sim \mathcal{N}\left(u_{\text{re/im}}, \frac{|g|^2\sigma^2}{2}\right)$.

The probability of a decision error towards the neighboring constellation point with a distance d according to Fig. 2 is obtained by integration over the area of the receive signal probability density function $f_{\hat{u}}(\hat{u}) = f_{\hat{u}_{\text{re}}}(\hat{u}_{\text{re}}) f_{\hat{u}_{\text{im}}}(\hat{u}_{\text{im}})$ causing the corresponding decision error.

For the one bit constellation, the probability of a decision error is given by

$$p_{\text{flip},1} = \int_{\hat{u}_{\text{re}}=-\infty}^{u_{\text{re}}-d/2} f_{\hat{u}_{\text{re}}}(\hat{u}_{\text{re}})\mathrm{d}\hat{u}_{\text{re}} = F_{\hat{u}_{\text{re}}}(u_{\text{re}} - d/2) \quad (10)$$

where $F_{\hat{u}_{\text{re}}}(\hat{u}_{\text{re}})$ is the cumulative density function of the receive signal real or imaginary part, assuming that $f_{\hat{u}_{\text{re}}}(\hat{u}_{\text{re}}) = f_{\hat{u}_{\text{im}}}(\hat{u}_{\text{im}})$ holds for the noisy receive signal.

For constellations with two or more bits, a symbol error may cause multiple bit flips. The 8 directly neighboring constellation points are considered to derive the bit error probability lower bound. As indicated in Fig. 2, there are two different error probabilities. $p_{\text{flip,face}}$ for the four closest points

$$p_{\text{flip,face}} = \int_{\substack{\hat{u}_{\text{re}}=u_{\text{re}}-3d/2\\ \hat{u}_{\text{im}}=u_{\text{im}}-d/2}}^{\substack{u_{\text{re}}-d/2\\ u_{\text{im}}+d/2}} f_{\hat{u}}(\hat{u})\mathrm{d}\hat{u}_{\text{re}}\mathrm{d}\hat{u}_{\text{im}} \approx p_{\text{flip},1} - 2p_{\text{flip},1}^2 \quad (11)$$

and $p_{\text{flip,diag}}$ for the diagonally neighboring constellation points according to [1]

$$p_{\text{flip,diag}} = \int_{\substack{\hat{u}_{\text{re}}=u_{\text{re}}-3d/2\\ \hat{u}_{\text{im}}=u_{\text{im}}-3d/2}}^{\substack{u_{\text{re}}-d/2\\ u_{\text{im}}-d/2}} f_{\hat{u}}(\hat{u})\mathrm{d}\hat{u}_{\text{re}}\mathrm{d}\hat{u}_{\text{im}} \approx p_{\text{flip},1}^2. \quad (12)$$

As shown in Fig. 2, the number of possible bit errors is different between the linear and modulo receiver because for the modulo receiver, constellation points may repeat outside of the square modulo region. Counting the average number of erroneous bits for a symbol error for the two different error probabilities $p_{\text{flip,face}}$ and $p_{\text{flip,diag}}$ gives the corresponding number of erroneous bits n_{face} and n_{diag} according to Tab. II. As a flip outside the constellation space does not cause a bit flip in the linear receiver, the values for the modulo reciever are higher than for the linear receiver.

$\hat{b}$	$n_{\text{face,lin}}$	$n_{\text{diag,lin}}$	$n_{\text{face,mod}}$	$n_{\text{diag,mod}}$
1	0.2500	0.5000	1.0000	0
2	0.5000	1.0000	1.0000	2.0000
3	0.8125	1.6250	1.5000	2.5000
4	1.0000	2.0000	1.5000	3.0000
5	1.5312	2.7656	1.6562	3.0469
6	1.3750	2.7500	1.7500	3.5000
7	1.6641	3.2539	1.7891	3.5039
8	1.6250	3.2500	1.8750	3.7500
9	1.7793	3.5381	1.8730	3.7256
10	1.7812	3.5625	1.9375	3.8750
11	1.8638	3.7219	1.9263	3.8469
12	1.8750	3.7500	1.9688	3.9375

TABLE II
AVERAGE NUMBER OF ERRONEOUS BITS PER SYMBOL ERROR

From Eq. (11), Eq. (12) and Tab. II, the uncoded bit error rate $p_{\text{error},\hat{b}}$ is

$$p_{\text{error},\hat{b}} = \frac{4n_{\text{face},\hat{b}}p_{\text{flip,face}} + 4n_{\text{diag},\hat{b}}p_{\text{flip,diag}}}{\hat{b}}. \quad (13)$$

Conversely, the required SNR $SNR_{\text{req},\hat{b}}$ can be defined as

$$SNR_{\text{req},\hat{b}} = \min SNR \text{ s.t., } p_{\text{error},\hat{b}}(SNR) \le p_{\text{error,target}} \quad (14)$$

Evaluating Eq. (14) for the G.fast constellations at $p_{\text{error}} = 10^{-7}$ gives the required SNR according to Tab. III.

[1]The exact solutions for the integrals of Eq. (11) and (12) would be $p_{\text{flip,face}} = p_{\text{flip},1} - 2p_{\text{flip},1}^2 - (p_{\text{flip},2} - 2p_{\text{flip},2}p_{\text{flip},1})$ and $p_{\text{flip,diag}} = p_{\text{flip},1}^2 - (p_{\text{flip},2}^2 - 2p_{\text{flip},2}p_{\text{flip},1})$ with $p_{\text{flip},2} = F_{\hat{u}_{\text{re}}}(u_{\text{re}} - 3d/2)$, but for the SNR region of interest, the difference between and the precise lower bounds can be ignored.

ISBN 978-0-9928626-7-1 © EURASIP 2017

bits	1	2	3	4	5	6
$SNR_{\text{req},\hat{b}}$ lin.	11.3	14.4	18.3	21.4	24.4	27.5
bits	7	8	9	10	11	12
$SNR_{\text{req},\hat{b}}$ lin.	30.5	33.6	36.5	39.6	42.4	45.6
bits	1	2	3	4	5	6
$SNR_{\text{req},\hat{b}}$ mod.	11.8	14.5	18.5	21.5	24.5	27.5
bits	7	8	9	10	11	12
$SNR_{\text{req},\hat{b}}$ mod.	30.5	33.6	36.5	39.6	42.4	45.6

TABLE III
SNR VS. BIT ALLOCATION TABLE FOR UNCODED TRANSMISSION

bits	1	2	3	4	5	6
$SNR_{\text{req},\hat{b}}$ lin.	5.4	8.4	12.7	15.8	18.9	22.1
bits	7	8	9	10	11	12
$SNR_{\text{req},\hat{b}}$ lin.	25.1	28.2	31.1	34.3	37.1	40.3
bits	1	2	3	4	5	6
$SNR_{\text{req},\hat{b}}$ mod.	6.8	9.2	13.2	16.1	19.0	22.3
bits	7	8	9	10	11	12
$SNR_{\text{req},\hat{b}}$ mod.	25.1	28.3	31.2	34.3	37.1	40.3

TABLE IV
SNR VS. BIT ALLOCATION TABLE FOR TRELLIS CODED MODULATION FROM HARDWARE DECODER MODELS

C. Trellis-Coded Modulation

G.fast uses forward error correction to reduce the bit error rates. The coding scheme used is the 4D-Wei-Code [3]. Only two LSBs of a constellation are protected, while the remaining bits pass through the trellis coder without changes. Two carriers are encoded jointly and build up a 4-dimensional constellation where one redundancy bit is added.

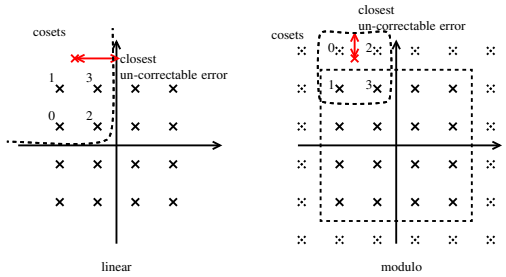

Fig. 3. Comparison of error regions for trellis coded modulation

As only two bit per constellation are protected, the Viterbi decoder at receiver selects the received constellation point out of four closest constellation points with different LSB values 0 to 3, called cosets (see Fig. 3). The selection of closest points on the boundary is different between linear and modulo receiver, causing the modulo loss for trellis coded THP.

Trellis coding gives a coding gain around $\gamma_{\text{coding}} = 5.2\,\text{dB}$. For the 12 bit constellation, there is almost no difference between linear and modulo receiver, while for the 2 bit constellation, there is a larger gap, representing the modulo loss. Trellis coding adds some redundancy. According to [9], the number of overhead bits N_{oh} per DMT symbol is given by

$$N_{\text{oh}} = \left\lceil \frac{N_{\text{used}} - N_{\text{single}}/2}{2} - 4 \right\rceil \tag{15}$$

where N_{used} is the number of used tones with bit allocation of 1 or more bits and N_{single} is the number of 1 bit carriers.

The required SNR for a certain bit allocation for trellis coded modulation is summarized in Tab. IV.

D. Reed-Solomon Coding and Interleaving

The G.fast link is additionally protected by configurable Reed-Solomon code with $32 \leq N_{\text{fec}} \leq 255$ bytes block size containing $2 \leq R_{\text{fec}} \leq 16$ overhead bytes. To correct error bursts caused by the trellis code, RS coding is combined with intra-DTU interleaving, where multiple RS code blocks are interleaved and combined to a DTU (data transmission unit). The required SNR for each constellation is shown in Tab. V for the linear as well as for the modulo receiver, using $N_{\text{fec}} = 255$ and $R_{\text{fec}} = 16$. The combination of RS and trellis coding achieves the target bit error rates at even lower SNR values and adds more transmission overhead.

bits	1	2	3	4	5	6
$SNR_{\text{req},\hat{b}}$ lin.	2.8	5.6	10.0	13.3	16.4	19.7
bits	7	8	9	10	11	12
$SNR_{\text{req},\hat{b}}$ lin.	22.6	25.8	28.7	31.9	34.8	37.9
bits	1	2	3	4	5	6
$SNR_{\text{req},\hat{b}}$ mod.	4.8	6.8	10.8	13.8	16.6	19.9
bits	7	8	9	10	11	12
$SNR_{\text{req},\hat{b}}$ mod.	22.7	25.9	28.8	31.9	34.8	37.9

TABLE V
SNR VS. BIT ALLOCATION TABLE FOR TRELLIS AND REED-SOLOMON CODING FROM HARDWARE DECODER MODELS

E. Theoretical Modulo Loss Model

Comparing Tab. III, IV and V indicates that the gap between the required SNR of linear and modulo receivers increases with increasing coding gain. The modulo loss γ_{modulo} for a given target bit error rate $p_{\text{error,target}}$ is given by

$$\gamma_{\text{modulo}} = \frac{SNR_{\text{req,mod},\hat{b}}(p_{\text{error,target}})}{SNR_{\text{req,lin},\hat{b}}(p_{\text{error,target}})}. \tag{16}$$

For uncoded modulation, Eq. (16) can be evaluated efficiently, as the required SNR for a certain target bit error rate can be derived from Eq. (14) and (13). Under the assumption that the modulo loss depends primarily on the receiver error variance $|g|^2\sigma^2$, the modulo loss for coded modulation can be approximated from the required SNR of the linear receiver by the following steps:

1) Determine the uncoded bit error probability $p_{\text{error,unc}}$ (linear receiver) which corresponds to the SNR $SNR_{\text{req,lin},\hat{b}}(p_{\text{error,target}})$ where coded modulation achieves the target bit-error rate (Eq. (13)).
2) Determine the required SNR $SNR_{\text{req,mod},\hat{b}}(p_{\text{error,unc}})$ for the modulo receiver for the same bit error probability.
3) Evaluate Eq. (16).

Fig. 4 compares the modulo loss, derived from the uncoded BER closed from equations (Eq. (13), (14) and (16)) with

ISBN 978-0-9928626-7-1 © EURASIP 2017

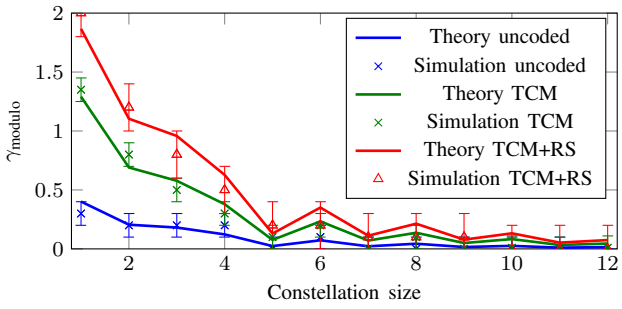

Fig. 4. Comparison between modulo loss model and the modulo loss derived from simulations

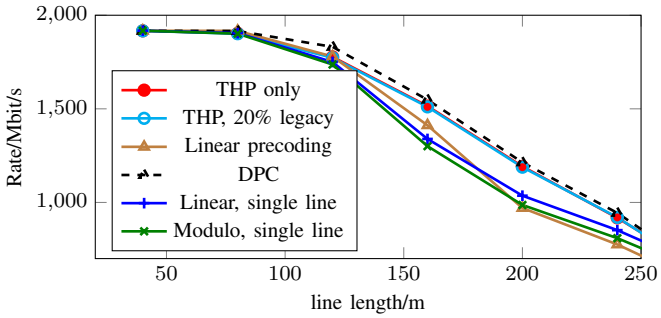

Fig. 5. Rate vs. reach comparison in crosstalk-free environment, linear vs. modulo receiver

the values derived from a bit error rate simulation. As the simulated target SNR values are determined from a hardware model which includes some implementation limitations, there is a ± 0.2 dB inaccuracy in the simulated modulo loss. Taking that into account, there is a good match between the theoretical results and the simulation.

V. Simulation Results

The effect of THP losses on the performance of a G.fast system is analyzed in terms of rate vs. reach simulations. Simulation conditions are 212 MHz G.fast with 4 dBm transmit power and 20 MHz start frequency. 20-pair cable binders with non co-located CPEs, randomly distributed between 10 m and 250 m distance to the DPU are assumed. Monte Carlo simulations with multiple cable binders are performed. The cable type is a DTAG 0.5mm PE cable (I-O2YS(ST)H) according to [10]. Reed-Solomon coding with 239/255 code rate and trellis coding is assumed. Background noise is -140 dBm/Hz below 30 MHz and -150 dBm/Hz above 30 MHz. Spectrum optimization according to [1] is applied.

Fig. 5 shows the rate vs. reach curves for various cases. Comparing the curves denoted as "single line", where modulo loss at the receiver and power loss at the transmitter are applied for a single line (no THP gain) indicates that THP losses account for 5% rate loss. In a more practical high crosstalk case, the performance gain of THP over linear precoding compensates the modulo losses. Fig. 5 shows the rate vs. reach curves for THP lines, only and THP lines in a mixed deployment with 20% legacy lines (randomly picked) in comparison with optimized linear zero-forcing precoding according to [1]. The DPC curve shows the remaining performance gap to nonlinear precoding without losses.

As Fig. 5 indicates, the performance advantage of THP over linear precoding is present in the given scenario for both, the THP only as well as the mixed case with some percentage of linear receivers in the binder. The reasons for the higher performance gap between LP and THP compared to earlier results, e.g., in [1] is the lower noise of -150 dBm/Hz at high frequencies and the increased start frequency of 20 MHz.

VI. Conclusion

Tomlinson Harashima precoding is investigated as an alternative precoding method for G.fast, while the THP losses and the actual performance advantage of THP over linear precoding is a topic for discussions, especially for the modulo loss. This paper presents a method to estimate the modulo loss for different coding schemes, based on SNR. No time consuming bit error rate simulations are required while the results are very similar to those from the BER simulation. The modulo loss analysis indicates that the modulo loss increases with increasing coding gain.

Support of legacy equipment is important to make THP systems deployable. This paper presents an approach which allows a mix of linear and modulo receivers. The THP performance gain slightly reduces for all lines in the binder, but the performance advantage of THP over LP is still present. Looking at the performance loss caused by a modulo receiver in a crosstalk free environment, the results indicate that modulo receivers may only be enabled in case of higher crosstalk, where the THP performance gain is sufficient. The presented approach of mixed precoding for linear and modulo receivers will allow to enable or disable the CPE-side modulo receiver on demand, while the precoder supports a mix of both.

References

[1] R. Strobel, A. Barthelme, and W. Utschick, "Zero-Forcing and MMSE Precoding for G.fast," in *2015 IEEE Global Communications Conference*, San Diego, USA, Dec. 2015.

[2] G. Ginis and J. Cioffi, "Vectored transmission for digital subscriber line systems," *IEEE Journal on Selected Areas in Communications*, vol. 20, no. 5, pp. 1085–1104, 2002.

[3] L.-F. Wei, "Trellis-coded modulation with multidimensional constellations," *IEEE Transactions on Information Theory*, vol. 33, no. 4, pp. 483–501, 1987.

[4] M. H. Costa, "Writing on dirty paper (corresp.)," *IEEE Transactions on Information Theory*, vol. 29, no. 3, pp. 439–441, 1983.

[5] W. Lanneer, M. Moonen, P. Tsiaflakis, and J. Maes, "Linear and nonlinear precoding based dynamic spectrum management for downstream vectored G.fast transmission," in *IEEE GLOBECOM 2015*, 2015.

[6] W. Yu, D. P. Varodayan, and J. M. Cioffi, "Trellis and convolutional precoding for transmitter-based interference presubtraction," *IEEE Transactions on Communications*, vol. 53, no. 7, pp. 1220–1230, 2005.

[7] J. Neckebroek, M. Moeneclaey, W. Coomans, M. Guenach, P. Tsiaflakis, R. B. Moraes, and J. Maes, "Novel bitloading algorithms for coded g. fast dsl transmission with linear and nonlinear precoding," in *International Conference on Communications (ICC)*. IEEE, 2015, pp. 945–951.

[8] J. Cioffi, "A multicarrier primer," *ANSI T1E1*, vol. 4, pp. 91–157, 1991.

[9] ITU-T Rec. G.9701, "Fast Access to Subscriber Terminals - Physical layer specification," ITU Recommendation, 2015.

[10] Broadband Forum, "TR-285 Cable Models for Physical Layer Testing of G.fast Access Network," Technical Report, 2015.

ISBN 978-0-9928626-7-1 © EURASIP 2017